Acta Geophys. (2017) 65:331–344
DOI 10.1007/s11600-017-0028-7

RESEARCH ARTICLE

Energy-based analysis of permanent strain behaviour of cohesive soil under cyclic loading

Wojciech Sas[1] · Andrzej Głuchowski[1] · Bartłomiej Bursa[2] · Alojzy Szymański[2]

Received: 30 December 2016 / Accepted: 10 March 2017 / Published online: 1 April 2017

Abstract In this paper the original results of uniaxial cyclic compression test on cohesive soil are presented. The shakedown phenomena in cohesive soil are described. Energy-based method highlights the change of soil material behaviour from plastic shakedown through plastic creep shakedown to incremental collapse. The samples were cyclically loaded under undrained conditions with the constant amplitude of stress in one-way test procedure. In this study the energy-based method was presented as a proper method to categorise response of cohesive soil to cyclic loading in uniaxial conditions. A shakedown criterion factor, S_E, was introduced to help understand the shakedown phenomena in cohesive soil. In cohesive soils the absence of a limit between plastic shakedown and plastic creep shakedown was pointed out.

Keywords Cohesive soil · Shakedown · Energy · Cyclic loading · Uniaxial compression · Soil mechanics

✉ Andrzej Głuchowski
andrzej_gluchowski@sggw.pl

Wojciech Sas
wojciech_sas@sggw.pl

Bartłomiej Bursa
bartlomiej_bursa@sggw.pl

Alojzy Szymański
alojzy_szymanski@sggw.pl

[1] Water Centre Laboratory, Faculty of Civil and Environmental Engineering, Warsaw University of Life Sciences – SGGW, Warsaw, Poland

[2] Department of Geotechnical Engineering, Faculty of Civil and Environmental Engineering, Warsaw University of Life Sciences – SGGW, Warsaw, Poland

Introduction

The behaviour of the soil under cyclic loading has been studied by many researches recently (Kokusho and Kaneko 2014; Feng et al. 2015; Cai et al. 2015; Sas et al. 2014, 2015). The most extensive studies were focused on liquefaction phenomena because of the danger that can be caused by its appearance (Kokusho and Kaneko 2014; Kokusho et al. 2012). One of the causes of liquefaction phenomena occurrence is the presence of high frequent cyclic loading which can be forced by traffic, earthquake or machinery vibrations. In opposite to this high frequent loading there also exists the slow quasi-static repeated loading excitated by, for instance, soil mass movements (there is no danger of liquefaction) (Zhou and Gong 2001). When it comes to cohesive soil the liquefaction phenomena does not exist. There is still a little knowledge about the cohesive soil behaviour under quasi-static cyclic loading. Quasi-static loading is characterised by time effect negligibility. In geotechnical field of studies such loading appears when its frequency is less than 2–5 Hz (Danne and Hettler 2015; Wichtmann 2005). The quasi-static phenomena occurs when harmonic excitation applied on a specimen causes displacement: $u = u^{ampl} cos(\omega t)$ with acceleration $\ddot{u} = -u^{ampl}\omega^2 \cos(\omega t)$, where $u^{ampl}\omega^2 << g$ (Danne and Hettler 2015).

Quasi-static loads are often encountered in industrial foundations, technical roads or local motorways. In the road engineering the effect of the cyclic loading can be observed as the rutting, and in foundation engineering it exists in the form of foundation settlement (Cuéllar et al. 2014; Kokkali et al. 2014; Soares et al. 2014). In the case of quasi-static loading the damage is not caused by the bearing capacity lost, but due to the plastic strain accumulation.

Among many types of soil, cohesive soil is merely examined by the researches; one of the reasons is that this type of soil is not often used as the bearing material. Nevertheless, the cohesive soil should be investigated because even the low stress level can cause high deformation which leads to weaken the above bearing layers. Therefore, engineers seek for the new design procedures which take into account the cyclic loading phenomena in cohesive soil (Soares et al. 2014; Lu et al. 2014).

Shakedown theory in soil mechanics is derived from the observations of the soil response to cyclic loading in various range of stresses (Goldscheider 1978). Shakedown theory has been used to explain the behaviour of engineering structures loaded with repetitive force. The pressure vessels under thermal cyclic loading problem were the first application of this concept, and later it was applied to the rolling on metal surfaces problem (König and Maier 1981). When it comes to geomechanics the shakedown theory was used in the road structures (Werkmeister et al. 2001; Werkmeister 2006; Tao et al. 2010; Nega et al. 2015; Sharp and Booker 1984; Boulbibane and Collins 2015).

The fundamental concept of shakedown theory is a division of the behaviour of the soil into five categories (König and Maier 1981):

- Purely elastic, where load is small enough to cause only the elastic strains. No plastic strains occur and response to cyclic loading is purely elastic (0).
- Elastic shakedown, where repeated loading causes plastic strains in the first cycles. After this phase, no further plastic strains occur and the material behave purely elastic. The maximum stress level when this phenomena occurs is called elastic shakedown limit (1).
- Plastic shakedown, where plastic strains occur, but after a few cycles material achieves steady hysteretic response. Nevertheless, the hardly noticeable small plastic strains can be observed. The maximum stress level when this phenomena occurs is called the plastic shakedown limit (2).
- Plastic creep shakedown, where after a few cycles the material hardens and the plastic strains occur (3).
- Incremental collapse, where the stress level causes accumulation of extensive plastic strains. The plastic strains in this stage cause cracks and the material degradation (4).

The shakedown concept typically defines the appropriate limit stress to prevent from excessive plastic strain (Fadaee et al. 2008). Settlement of subgrade soils is adverse because it mostly leads to road damage. The excessive settlement of subgrade soils is typically caused by the accumulation effect from traffic load. The repeated stress and strain will not completely dissipate in the unloading state and will accumulate and transfer along road structure to subgrade layer (Puppala 2009).

Conducted tests with shakedown application mostly concern unbound granular material (UGM) testing. The shakedown concept is utilised as a method of permanent strain behaviour analysis. The shakedown theory is now utilised in permanent strain evaluation for UGM and the procedure of shakedown analysis for this materials is standardised and presented in European Standards: EN 13286–7 (2004; Cerni et al. 2012). The shakedown concept in applications in transportation geotechnics mostly concerns cyclic compression (Soliman and Shalaby 2015). Shakedown concept was utilised for study of fine addition to UGM. The resistance of material to permanent deformation for UGM and non-cohesive soils was linked to shear strength of material. The slip between particles under traffic loading was recognised as most sensitive phenomenon which triggers permanent deformation occurrence (Soliman and Shalaby 2015).

Under cyclic loading the same response can be observed in cohesive as well as non-cohesive soil. A mechanism is similar (rolling and sliding of grains develop plastic strain), but in addition in cohesive soil the cohesion forces counteract the development of the plastic strains (Chen et al. 2015; Karg et al. 2010). Identification of this mechanism is very complicated and time-consuming, so the simplified methods are usually employed for analysis. One of the branches of the simplified methods is energy-based method which is utilised in many fields of applied mechanics, especially when it comes to cyclic and dynamic loading (Liang et al. 2015; Seo et al. 2015). This method is based on the first law of thermodynamics (assuming the negligibility of kinetic energy) and tells that all external forces transform into internal energy and are dissipated in the form of the plastic strains. Using energy-based method we were able to categorise a response of a material to one of the shakedown categories. In this paper a new proposition of the energy-based method application is proposed.

Studies under clayey subsoil traffic-load-influenced depths employed shakedown concept to distinguish three depths of cyclic traffic load influence: the threshold depth beyond which traffic loads becomes negligible, the plastic shakedown limit depth where subgrade experiences continuous deformation and the critical failure depth where subsoil will fail due to excessive strain (Tang et al. 2015).

The studies on effects of cyclic confining pressure on the deformation characteristics of natural soil have found that the shapes of all hysteresis loops looks similar in general. But with the number of cycles, the increment of residual axial strain caused by a single cycle is reducing gradually (Sun et al. 2015), which may be classified as plastic shakedown.

Other studies concerning low frequent cyclic loading, cyclic loading in consolidometer or in variable confining pressure mention the decrease on plastic strain rate during cyclic loading which again may be related to shakedown concept (Cai et al. 2013; Kalinowska and Jastrzębska 2014; Li et al. 2011; Gu et al. 2012). Therefore, simple criterion of distinguishing the permanent strain accumulation phenomena in cohesive soil is needed for proper classification of plastic strain development.

Materials and methods

Materials

In this study the cohesive soil material obtained from 2 m deep earthwork was analysed. The samples of this material were remoulded and tested physically and mechanically. Table 1 presents results of mechanical and physical properties of material used in this study.

Based on sieve test (PKN-CEN ISO/TS 17892-4:2009) with respect to Polish standards (PN-EN ISO 14688-2:2006), tested soil was recognised as sandy clay (saCl).

Soil material before main tests was prepared with respect to the Proctor method. This procedure leads to establish constant test conditions (constant moisture and maximum dry density). The undisturbed samples were first dried and ground to powder. The material was next compacted at optimum moisture content with respect to the Proctor energy of compaction. The data about optimum moisture and maximal dry density were gathered by previous Proctor's test with respect to (PN-EN 13286-2:2010/AC). The abovementioned conditions are as follows: optimum moisture content, wopt. 10.5%, volume density maximum dry density ρ_s 2.15 g/cm^3.

The compaction of the samples was performed by rescaling the Proctor hammer with diameter of 3.5 cm and mass equal to 500 g. The sample dimensions were as follows: 7 cm diameter and 14 cm high. The clay powder was mixed with water with respect to optimum moisture content.

Table 1 Physical and mechanical properties of sandy clay in this study

Properties	Symbol	Value
Specific density of soil	ρ_s (g cm^{-3})	2.66
Maximum dry density	ρ_d (g cm^{-3})	2.15
Natural moisture	w_n (%)	12.82
Optimal moisture	w_{opt} (%)	10.5
Liquid limit	w_l (%)	37.4
Plasticity limit	w_p (%)	12.3
Plasticity index	I_p (–)	25.1
Void ratio	e_0 (–)	0.41

Methods

The tests of uniaxial cyclic loading were performed with Instron's loading frame where axial stress and displacement were registered. One series of ten tests was performed. Table 2 presents the parameters of each test in constant frequency equal to 0.1 Hz.

Uniaxial cyclic loading tests were performed using one-way loading test method without reversion of its direction. A sample was placed on a base and a rigid cap was placed on a top. The sample was covered by a rubber membrane to prevent moisture loss during a test. In Fig. 1a a schema of the uniaxial cyclic test is presented.

The one-dimensional tests are widely used in field of geotechnical engineering where comparative or preliminary studies can highlight material properties or non-traditional materials have not been tested (Koseki et al. 2014). The soil samples with "A" index represent high amplitude of cyclic loading. The samples with "B" index denote collapsed specimens and "C" index presents samples loaded by repeating stress with small amplitude. The cyclic stress can be characterised by five parameters which are maximal stress σ_{max}, minimal stress σ_{min}, stress amplitude σ_a, stress median σ_m and stress difference $\Delta\sigma$. Those stress values can fully describe repeated loading of any material (Jain et al. 2015). Figure 1b presents schematic stress–time curve with highlighter above-mentioned stress values. Table 3 presents detailed stress values for each test.

Energy density calculations

The results of the tests were later analysed by calculating the area of plastic energy density (dE^P) and elastic energy density (dE^E). The calculations were performed by

Table 2 Parameters of uniaxial cyclic loading test for tested samples

Sample	σ_{max} (kPa)	CSR (–)	No. of cycles
A.1	39.0	0.17	500
A.2	116.9	0.50	1000
A.3	142.9	0.61	2000
A.4	153.1	0.65	100
B.1	194.9	0.83	11
B.2	168.9	0.72	8
C.1	118.2	0.53	10,000
C.2	134.4	0.61	10,000
C.3	134.4	0.61	10,000
C.4	156.9	0.70	10,000

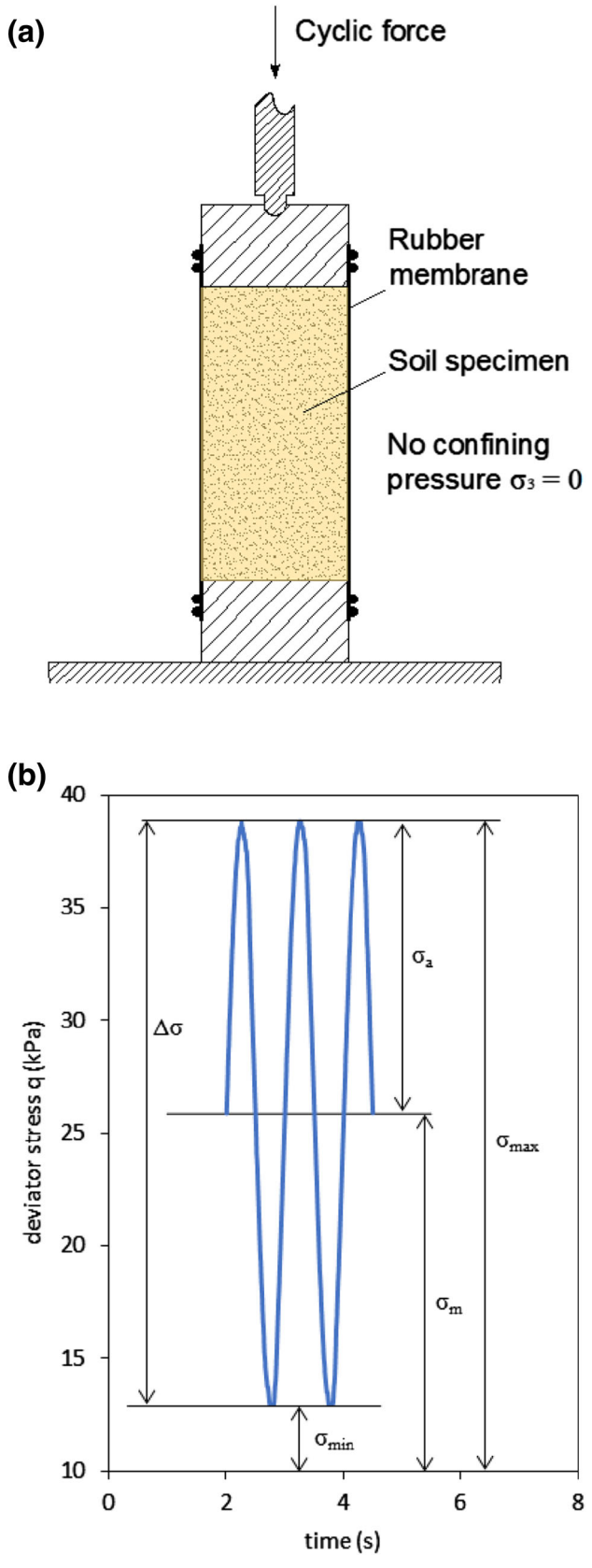

Fig. 1 The methods in this study: **a** schema of the uniaxial cyclic test, **b** schema of the stress characteristic values

Table 3 Stress characteristic values for uniaxial cyclic loading in this study

Sample	σ_{min}	σ_{max}	σ_a	σ_m	$\Delta\sigma$
A.1	13.0	38.8	12.9	25.9	25.8
A.2	13.2	65.4	26.1	39.3	52.2
A.3	16.5	145.9	64.7	81.2	129.5
A.4	16.7	150.1	66.7	83.4	133.4
B.1	16.5	194.9	89.2	105.7	178.4
B.2	16.5	168.9	76.2	92.7	152.4
C.1	94.3	118.2	11.9	106.3	23.8
C.2	121.5	134.4	6.4	128.0	12.9
C.3	121.5	134.4	6.4	128.0	12.9
C.4	134.5	156.9	11.2	145.7	22.4

Mathematica software where the self-made algorithm of the area calculation was employed.

The energy concept has been utilised in many fields in theory of plasticity and elasticity. Many constitutive laws and energy principles are based on energy concept (Desai and Siriwardane 1984; Pasik et al. 2015; Panoskaltsis and Bahuguna 1996). The energy-based methods can be divided into two categories: stress methods and strain methods. In the stress methods, the amount of strain energy is calculated from recorded stress and strain data during cyclic uniaxial loading. A hysteresis loop can be plotted from stress–strain data (Daum 2008). Figure 2 presents a typical hysteresis loops obtained from the cyclic compression loading from the stress-controlled cyclic uniaxial test.

The plastic strain energy density is equal to the area inside of hysteresis loop, and elastic energy density is equal to area under unloading curve (Ostadan et al. 1996; Green et al. 2000). In this study the plastic strain accumulation and elastic strain evolution are changed to equivalent plastic and elastic energy density to study changes of aforementioned strains during cyclic compression test. Plastic strain accumulation would be not observed between two next cycles, which was previously confirmed (Karg et al. 2010). The plastic energy density is, therefore, more sensitive to changes of soil sample behaviour during repeated loading. In Fig. 2, dE^P decreases rapidly and dE^E decrease is steady. The decline value of dE^P is represented by area of hysteresis loop reduction. Reduction of dE^E value with number of cycles represents the reduction of inclination of the hysteresis loop towards strain axis. The phenomena of dE^E decreasing indicate that the stiffness of the specimens tends to decrease. The dE^E descent has also impact on plastic strain accumulation and needs to be taken into consideration of plastic strain development.

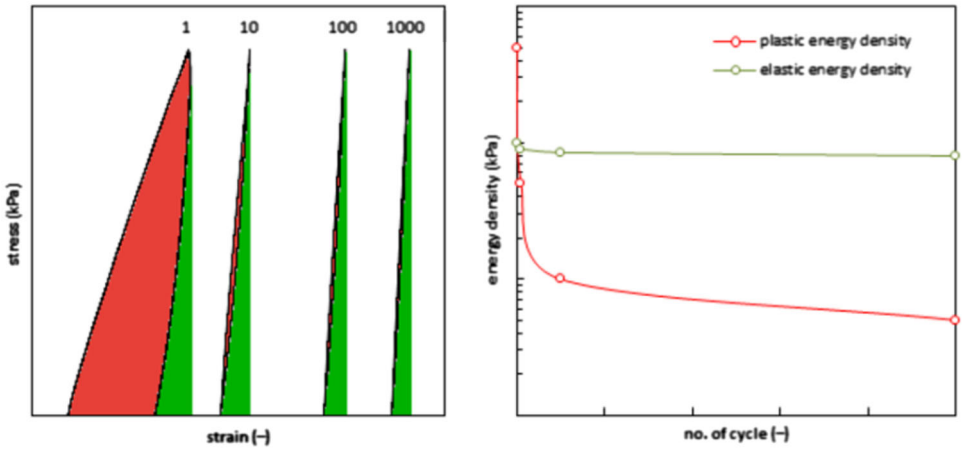

Fig. 2 Schema of the energy calculation for cyclic loading in this study

Results and discussion

Uniaxial cyclic test results

The results of the experiment were focused on the change of the energy densities during uniaxial cyclic compression loading. The results of uniaxial cyclic compression loading tests are presented in Figs. 3, 4 and 5. In Fig. 3 the results of the four tests from A.1 to A.4 are presented with stress–strain axis to study the shakedown concept. The plot presents hysteretic loops among different cycle numbers in test with the same stress conditions. Figures 3 and 5 show that with number of cycles the hysteresis loop inclination towards the X-axis tends to increase.

During cyclic loading, each sample was loaded to different amplitude of stress. For sample A.1 where axial of maximal stress σ_{max} was equal to 39.0 kPa plastic strain increment $\Delta\varepsilon_p$ after 500 cycles was equal to 0.0001034 (0.01034%).

For samples A.2, A.3 and A.4 the axial maximal stress was equal to 116.9, 142.9 and 153.1 kPa, respectively, and the plastic strain increment $\Delta\varepsilon_p$ was equal to 0.000416, 0.000401 and 0.000675, respectively.

Under higher maximal stress values (168.9 for B.2 and 194.9 kPa for B.1), the incremental collapse occurred. Standard uniaxial compression test has shown maximal strength of material σ_{max} 223.8 kPa which is 0.87 and 0.75 of maximum stress applied in tests B.1 and B.2, respectively (Fig. 4).

The samples B.1 and B.2 were destroyed during the tests. It was noticed that the last cycle before the collapsing was different from previous ones, and the crossing of the loading–unloading curves occurred in the lower stress level than in the previous cycles which may indicate the softening behaviour of the material.

The stress values characteristic parameters differed for samples "A" and "C". The amplitude of loading and stress median change results in another response of soil to repeated loading. For these samples, the decrease of axial stress was noted. The stiffness reduction was caused by characteristic stress conditions which differ from the test conditions in "A" phase of tests. This means that higher axial stress median is the higher stiffness reduction will occur (see Fig. 5).

In Fig. 6 a plot of the plastic strain increment during cyclic loading is presented, where various responses to cyclic loading can be distinguished. In a sample A.1 the plastic shakedown response to repeated loading can be noticed. In samples A.2 and A.3 at first the plastic shakedown response can be noticed as well, but after 100 repetitions the plastic strain tends to increase and, therefore, the plastic shakedown creep response occurs. The response of sample A.4 can be categorized as plastic creep shakedown. The characteristic of the curve from Fig. 4 is similar to the incremental collapse response, but the material was not destroyed. It may be caused by insufficient number of cycles that was programmed.

Samples B.1 and B.2 after a few cycles of loading collapsed due to accumulation of excessive plastic strains caused by strain softening. The response of the material can be categorised as incremental collapse.

Samples C.1 and C.3 follow the same pattern as samples A.2 and A.3. The plastic strain tends to stabilise and plastic shakedown occurs.

The plastic strain rate versus number of cycle for samples A.1–A.4 changes with logarithm of cycles. The decrease of plastic strain can be distinguished for samples from A.1 to A.4; nevertheless, the rate of this decrease in terms of shakedown criterion proposed by Werkmeister (2003) cannot be included in plastic shakedown response. The Werkmeister proposition consists of the accumulated permanent deformation analysis between 3000 and 5000 cycles. The proposition of such permanent strain accumulation analysis was established based on testing program of UGM (EN 13286-7:2004).

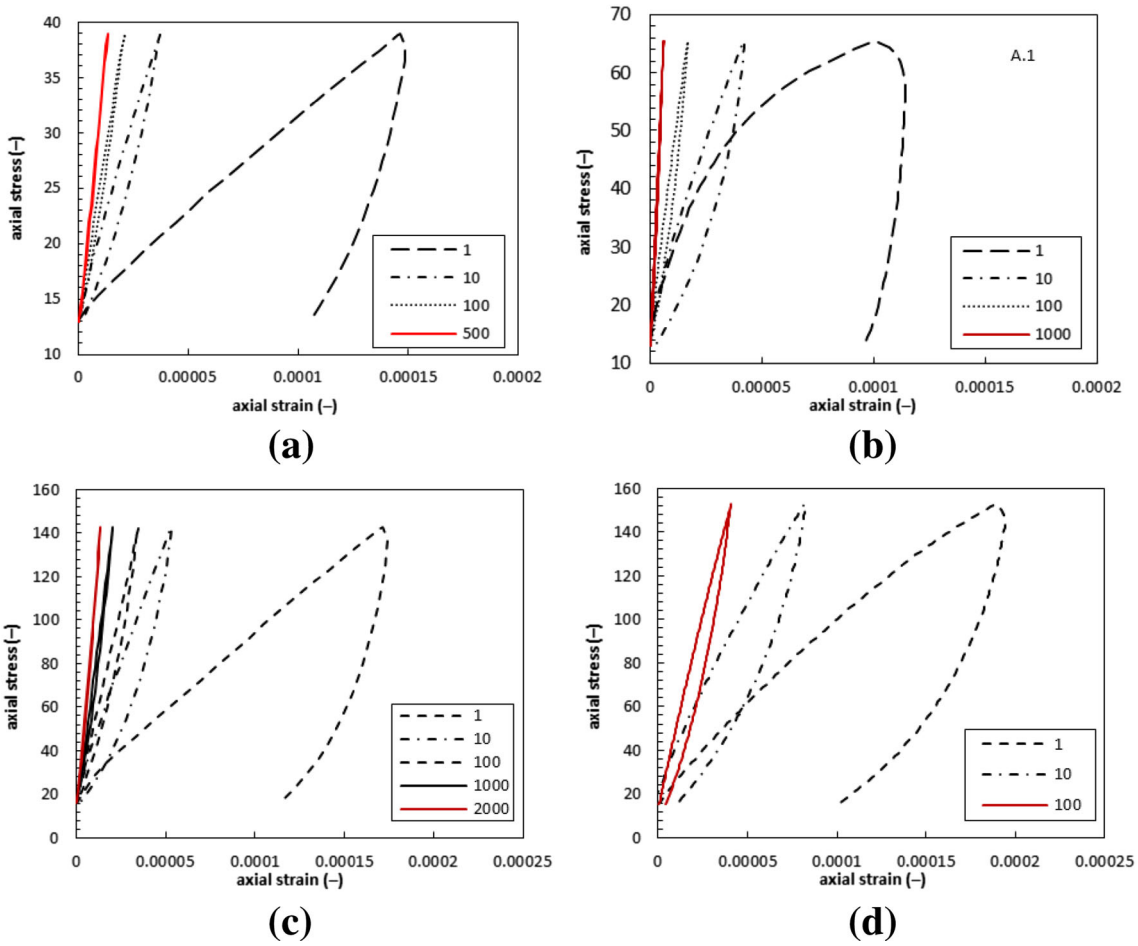

Fig. 3 Plot of the axial stress–strain for uniaxial cyclic loading of sandy clay in various stress levels—shakedown concept test (**a** A.1, **b** A.2, **c** A.3, **d** A.4), comparison of hysteretic loops among different cycle numbers

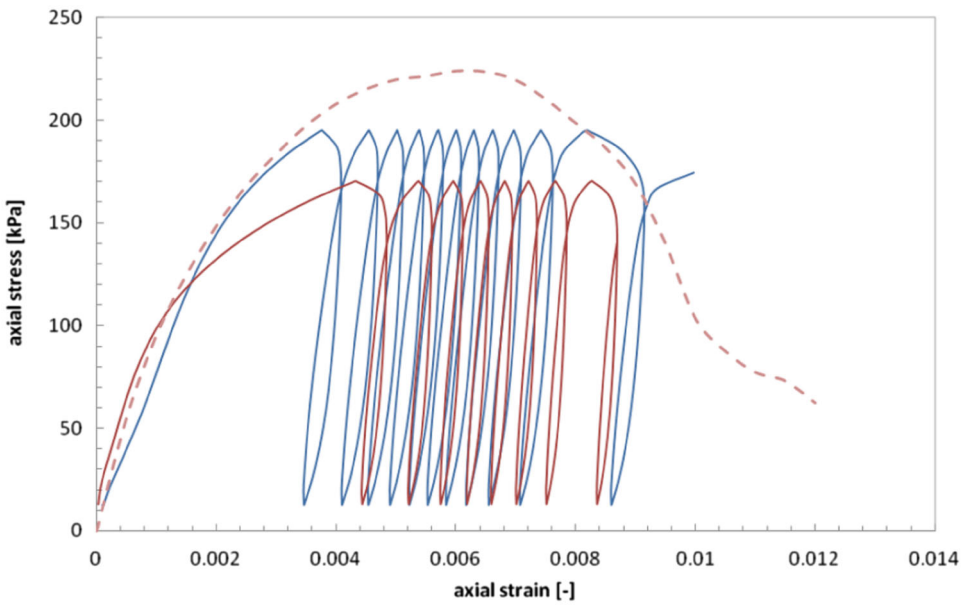

Fig. 4 Plot of the axial stress–strain for uniaxial cyclic loading of sandy clay in various stress levels—incremental collapse tests (*red* B.1, *blue* B.2, *dashed line* standard uniaxial compression test result)

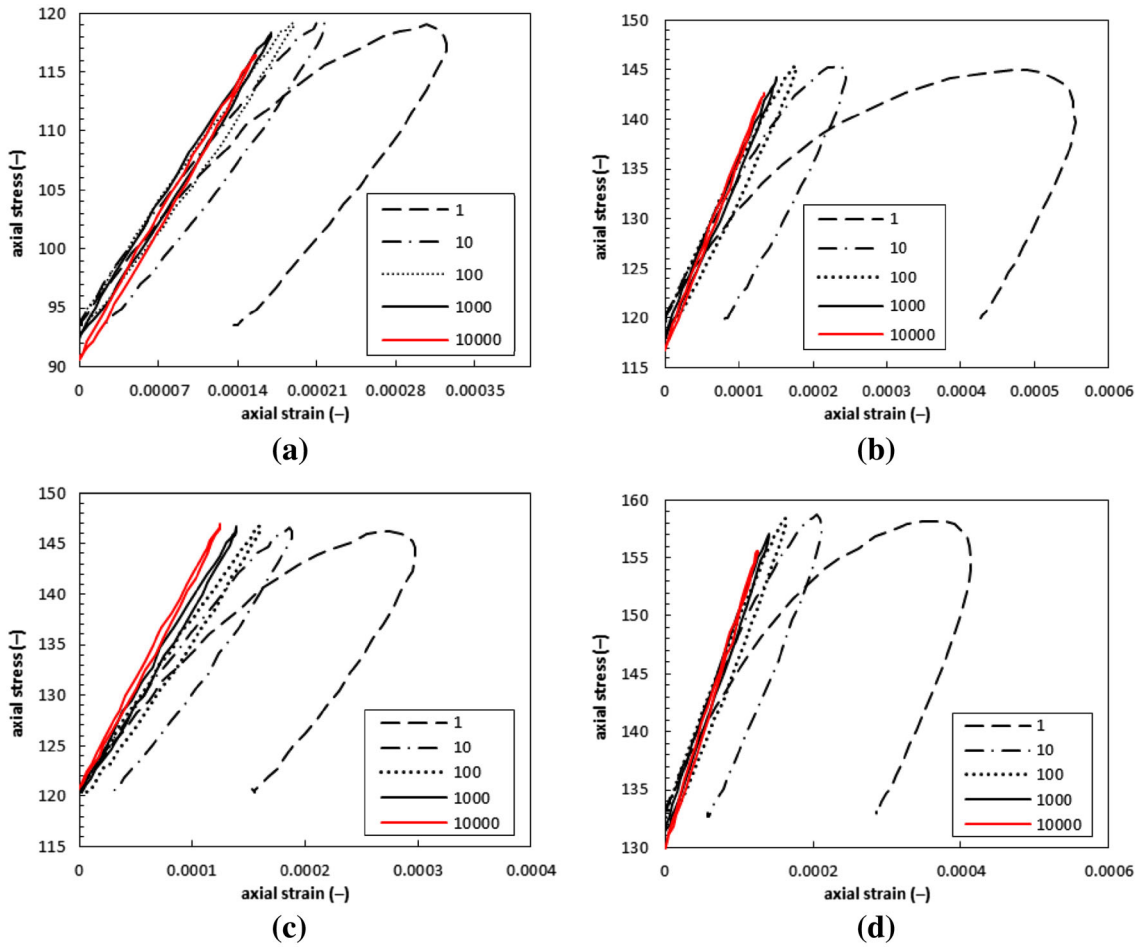

Fig. 5 Plot of the axial stress–strain for uniaxial cyclic loading of sandy clay in various stress levels—plastic creep concept (**a** C.1, **b** C.2, **c** C.3, **d** C.4), comparison of hysteretic loops among different cycle numbers

Aforementioned plastic shakedown limit is presented by Eq. (1):

$$\varepsilon_{p5000} - \varepsilon_{p3000} < 0.4 < 10^{-3} \quad (1)$$

If the difference between 5000 and 3000 cycle is less than $0.4 \cdot 10^{-3}$, then plastic shakedown occurs; if the difference crosses this limit, plastic shakedown creep occurs.

Plastic strain rate analysis presented in Fig. 6 for "C" indexed samples leads to estimate the shakedown response based on the Werkmeister proposition. The C.1 specimen difference between 5000th cycle and 3000th cycle is equal to $0.2 \cdot 10^{-3}$. The samples C.2, C.3 and C.4 were classified to plastic creep shakedown response and the difference was equal to $0.43 \cdot 10^{-3}$, $0.54 \cdot 10^{-3}$, $0.494 \cdot 10^{-3}$.

Energy calculation results

Figure 7a presents the energy calculation for the results of cyclic loading for A.1 sample. During cyclic loading drop of the dE^{P} (plastic energy density) can be observed. First loading caused the plastic strain equal to over 40% of all registered plastic strains in this study. It can be noticed that the dE^{E} does not change so drastically as the dE^{P}.

Figure 7b presents the energy calculation for the results of A.2 sample. In this plot it can be observed that in the beginning of the test the dE^{P} is close to A.1 sample (0.108 for A.1 and 0.0303 for A.2 sample). After 205 repetitions for A.1 sample dE^{P} was lower than 0.0001. In case of A.2 sample the same dE^{P} value occurred after 957 cycles. The differences between dE^{P} evolution means that the dE^{P} in sample A.2 decrease faster than in sample A.1 which can be understood as the huge decrease of the plastic strain rate.

Sample A.3 (Fig. 7c), where 2000 cycles were applied, behaves similar to A.2. In the specimen A.3 the initial value of dE^{P} is lower than in A.2 sample. It can be seen that dE^{E} is greater than dE^{P} from the beginning. This behaviour was different from A.2 and A.3 where at the beginning dE^{P} is greater than dE^{E}. The dE^{P} decreases steadily and the

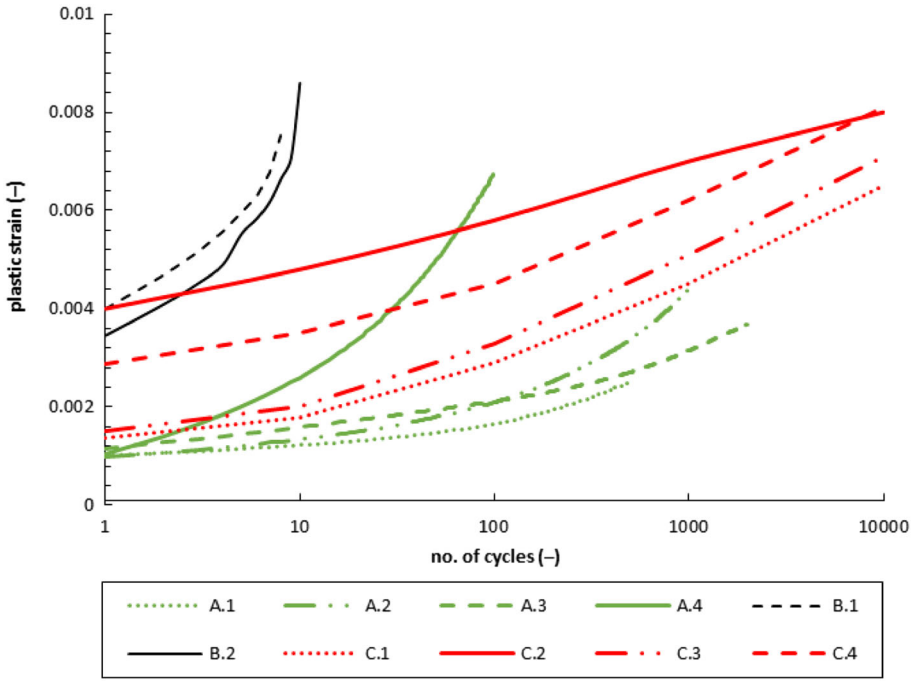

Fig. 6 Plot of the plastic strain from uniaxial cyclic loading of sandy clay vs. logarithm of number of cycles. (*Green* "A" indexed tests, *black* "B" indexed tests, *red* "C" indexed tests)

instant drop of this energy density was not noticed as it was in the previous samples.

Figure 7d presents the results of cyclic loading for sample A.4. The amplitude of the axial stress was equal to 153.1 kPa which was 0.68 of the maximum stress from the static uniaxial compression strength test. The beginning of the test was similar to A.3 sample. The dE^{P} decreases in the same way as in the sample A.3. The dE^{P} in the first two cycles was greater than the dE^{E}.

Figure 7e, f presents the results of the tests of B.1 and B.2 samples, respectively. For both of the specimens incremental collapse occurs after eight and 12 cycles, respectively. In both tests, the dE^{P} density is greater than the dE^{E} during the whole test. Before the collapse, the samples start to experience more plastic strain and the softening phenomena can be observed.

The samples from C.1 to C.4 present similar respond to cyclic loading (Fig. 7g–j). The stress amplitude and stress difference for these samples were close with the values. The plastic energy density drops after few first cycles.

Similar result was observed in the case of sample A.1. The A.1 sample characterizes with stress amplitude equal to 12.9 kPa, and the σ_a value for samples C.1 and C.4 was equal to 11.9 kPa and 11.2 kPa, respectively. Figure 8 presents comparison between A.1 and C.1 sample energy calculation. The energy density change during cyclic loading for both cases is very similar. Figure 10b presents comparison of plastic and elastic energy density between A.1 and C.1 specimens. The linear function was fitted to these relationships. The coefficient of determination R^2 for plastic energy density function was equal to 0.9388, and for elastic energy density the R^2 value was equal to 0.9042. The conclusion can be drawn that for close stress amplitude and stress difference values the energy density change is similar.

Results of energy calculation discussion

Accumulated plastic energy density

Figure 9 presents the change of accumulated dE^{P} during cyclic loading in various axial stress amplitude σ_{max}. It can be seen that after some value of axial stress the accumulated dE^{P} function changes its rate from the small rate in the beginning to higher rate after exceeding some σ value. Accumulation of the dE^{P} change can be explained by the fact of elastic and dE^{P} quotient. From the previous Figs. (7a–j, 8a–b), a conclusion was drawn that when the dE^{P} is closer to the dE^{E}, the bigger plastic strain occurs. From Fig. 9 it can be seen that after exceeding some σ value the accumulated dE^{P} density changes its rate. The higher the axial stress, the higher the accumulation of dE^{P}. This change of behaviour corresponds to a limit between plastic shakedown and plastic creep shakedown. Nevertheless, this limit is hard to estimate due to a lack of clear deflection point and its development in following cycles.

Determination of shakedown response from energy densities

Werkmeister et al. (2001) conducted studies on the responses of unbound aggregates subjected to cyclic

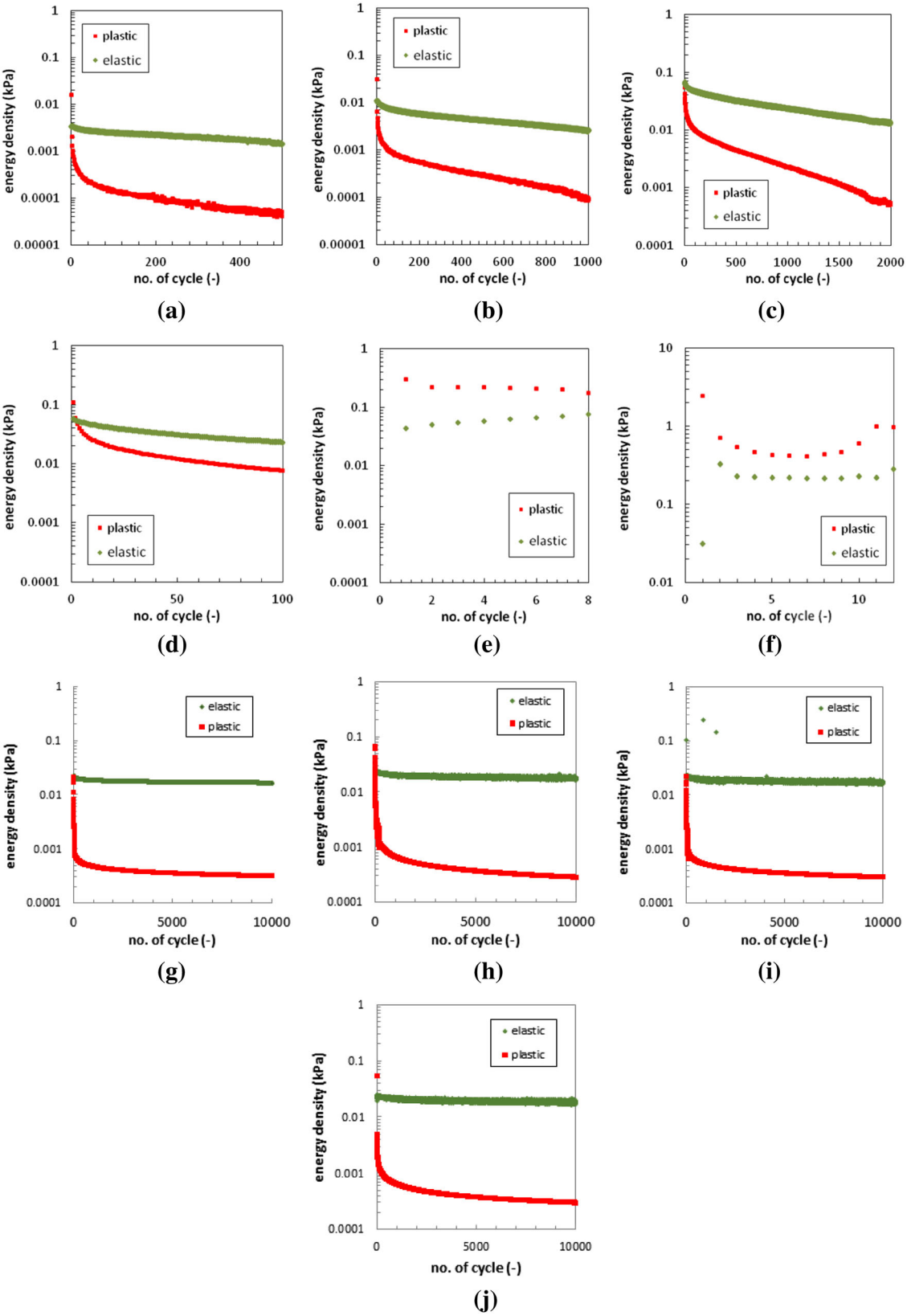

Fig. 7 Plot of the energy density versus number of cycles uniaxial cyclic loading of sandy clay in various stress levels (**a** A.1, **b** A.2, **c** A.3, **d** A.4, **e** B.1, **f** B.2, **g** C.1, **h** C.2, **i** C.3, **j** C.4)

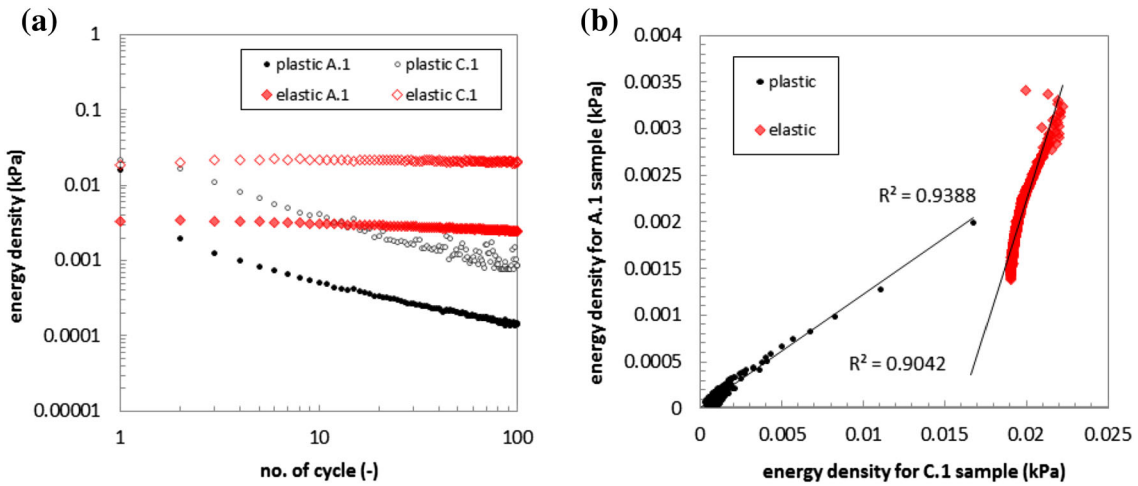

Fig. 8 Plot of the comparison of plastic and elastic energy density for samples A.1 and C.1

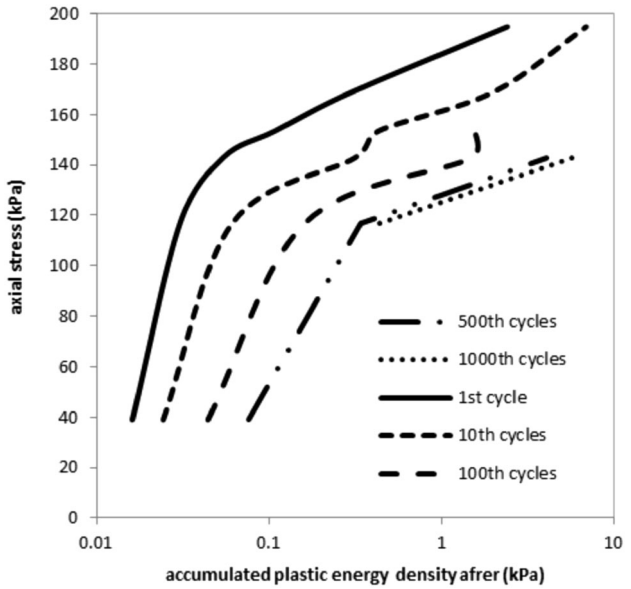

Fig. 9 Plot of accumulated plastic energy after first, tenth, 100th, 500th and 1000th cycle versus axial stress from uniaxial cyclic loading of cohesive soil

loading, which resulted in the proposition of the three ranges of response:

- Range A—plastic shakedown category; the response is plastic only for a first cycles of load and becomes resilient after the post–compaction. The accumulation of permanent strain decreases rapidly to a very small level,
- Range B—plastic creep shakedown category; the level of the plastic strain rate decreases to a low and nearly constant level during the first loading cycles,
- Range C—incremental collapse category; the accumulation of the plastic strain decreases slowly or does not.

Figure 10 presents an adjustment of shakedown criterion concept for cohesive soil based on proposition by Werkmeister (2006). The plot of normalized number of permanent strain versus number of cycles was calculated from the plastic strain rate analysis presented in Fig. 6. The exponential function's coefficient of determination of R^2 for samples A.1–A.4 was equal to 0.97 or higher. For cycle 3000 and 5000 plastic strains' difference based on Eq. 1 was calculated. Samples A.1 and A.3 were included in plastic shakedown range. Samples A.2 and A.4 were included in plastic creep shakedown range.

The proposition of the quotient of plastic and elastic energy dE^P/dE^E can help to understand the shakedown phenomena and plastic strain development in cohesive soil. In cohesive soil, limits of those three ranges are not clear as in the case of non-cohesive soil. The limit between the plastic shakedown and plastic creep shakedown ranges is not sharp and, therefore, the response of cohesive soil to cyclic loading is more fluent. The decrease of the plastic strain in low stress conditions is characterized by low dE^P in first cycles and by the fast decrease in further cycles. When stress level is greater, the initial dE^P is also bigger but a drop in dE^P value is lower. The plastic shakedown creep occurs when the abovementioned drop of dE^P is not presented; in other words, the decrease of the dE^P is constant. This causes greater plastic strain accumulation in the first few cycles and the creep phenomena in the next stage. When dE^P is big enough like in the case of high stress level, it may lead to incremental collapse even if the drop of its rate is observed.

The stress characteristic parameters such as stress amplitude and stress difference have their impact on the energy density change and, therefore, on strain development. The problem of cyclic stress impact on behaviour of

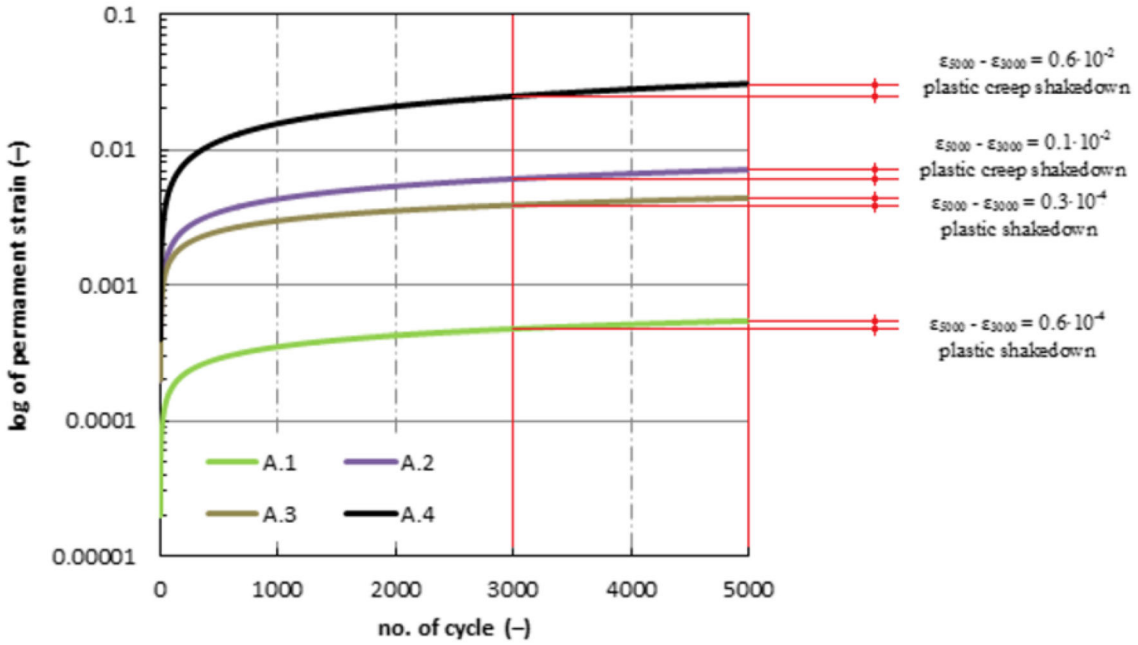

Fig. 10 Plot of shakedown criterion based on the Werkmeister proposition

soil can be resolved by including the stress parameters in energy calculations.

The plastic strain development during cyclic loading can be described by proposed in following Eq. (2) SE factor. The SE factor takes into account the shakedown concept and stress parameters: stress amplitude and stress median recognised as the cause of soil stiffness loss:

$$\left(\frac{\sigma_a}{\sigma_m}\right) \cdot \log\left(\frac{dE^P}{dE^E}\right) = S_E \tag{2}$$

The S_E factor value versus number of cycles is presented in Fig. 11. The cohesive soil can behave in plastic creep shakedown manner at the beginning of the test and later the response shifts to plastic shakedown. In range A, plastic strain can occur, but after numerous repetitions. In other words, the plastic strain could not be observed between two cycles but between 50 and 100 cycles. If the amplitude of axial stress increases, the dE^P approaches the dE^E and more plastic strain can be observed. If the amplitude of axial stress is big enough or in other words, the dE^P is nearly the same as the dE^E, the plastic strains occur in every cycle and plastic creep shakedown can be recognized. If the amount of dE^P is greater than dE^E, the plastic strain begins to increase in fast rate and incremental collapse can be observed.

In Fig. 11 it can be seen that incremental collapse occurs when the S_F is greater than 0. This corresponds to the range C from the Werkmeister proposition. Plastic creep shakedown occurs when value of S_F is between 0 and −0.25. When $S_F < -0.25$ plastic shakedown occurs.

Similar proposition of energy calculation was developed for hot-mix asphalt (HMA). The principle of this mechanism was describing of the fracture properties of HMA. In this framework, upper and lower thresholds, namely dissipated creep strain energy (DCSE) and fracture energy (FE), were distinguished. The DCSE limit is bound with continuous repeated loading and FE limit is associated with fracture of the HMA with a single application (Zhang et al. 2001; Birgisson et al. 2007; Tasdemir et al. 2010). When the energy threshold is exceeded, non-healable macrocracks develop and propagate along the mixture. Under this energy threshold, the rate of damage is governed by the creep properties of the mixture.

Conclusions

In this paper, cyclic uniaxial tests on cohesive soil were conducted to characterise shakedown phenomena. The test results were later analysed by application of the energy-based method. Based on the experimental results the following conclusions can be drawn:

1. During the uniaxial cyclic loading tests, the three ranges of the shakedown behaviour were observed which depended on the stress amplitude level. For the plastic shakedown response, rapid decrease of the dE^P and steady decrease of the dE^E were recognised. This behaviour results in small or in the lack of plastic strain

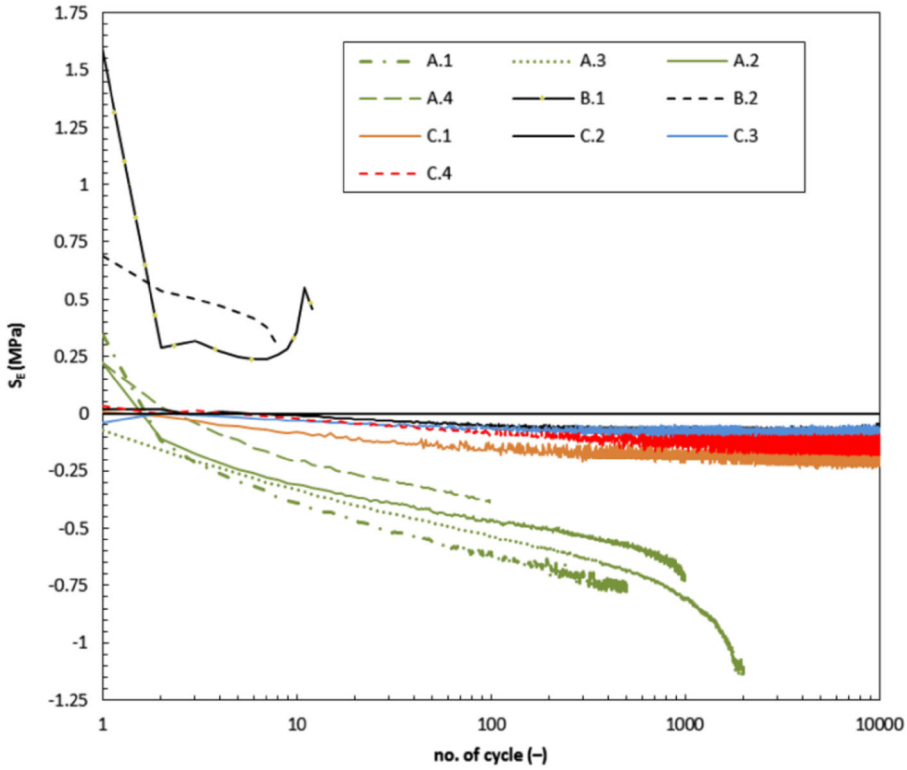

Fig. 11 Plot of S_E factor versus number of cycles

occurrence. For plastic creep shakedown a range of the dE^P decrease was less rapid, and the dE^E decreased more than that in plastic shakedown case. When the value of the dE^P decrease is near the dE^E, plastic creep shakedown may occur. Incremental collapse occurs when the dE^P is greater than the dE^E in all cycles which leads to failure.

2. Accumulated dE^P depends on the axial stress amplitude. This relation in non-linear and some inflection areas were recognised. These areas represent possible change of behaviour. Cohesive soil can behave as the plastic creep shakedown, but after numerous repetitions it may change to plastic shakedown.
3. A new proposition of distinguishing shakedown ranges for cohesive soil was proposed. The presented method bases on the ratio of plastic to dE^E and helps to recognise shakedown categories.
4. Energy-based method leads to the identification of smooth limit between plastic shakedown and plastic creep shakedown. The cohesive soil can behave in both ways which depend on the stress amplitude levels and the plastic and dE^E during cyclic loading.
5. Shakedown limit determination was performed with the calculation of the value of S_F. When the $S_F \geq 0$ the incremental collapse occurs. When $-0.25 \leq S_F < 0$ cohesive soil behaves as the plastic creep shakedown. When $S_F < -1$ the plastic shakedown may occur.
6. Cohesive soil subjected to cyclic loading behaves differently comparing to non-cohesive soil. The limit between the plastic shakedown and the plastic creep shakedown range is smooth and changes during cyclic loading. It may by possible that after post-compaction stage, the response can change due to fatigue of the material.
7. The practical application of the common logarithm of energy density quotient can lead to estimate maximal amplitude of cyclic loading which can improve pavement and foundation design process.

References

Birgisson B, Sangpetngam B, Roque R, Wang J (2007) Numerical implementation of a strain energy-based fracture model for a HMA materials. Int J Road Mat Pavement Des 8(1):7–45. doi:10.1080/14680629.2007.9690065

Boulbibane M, Collins IF (2015) Development Of A pavement rutting model using shakedown theory. Int J Pavement Eng Asph Technol 16(1):55–65. doi:10.1515/ijpeat-2015-0003

Cai Y, Gu C, Wang J, Juang CH, Xu C, Hu X (2013) One-way cyclic triaxial behavior of saturated clay: comparison between constant and variable confining pressure. J Geotech Geoenviron Eng 139(5):797–809. doi:10.1061/(ASCE)GT.1943-5606.0000760

Cai Y, Sun Q, Guo L, Juang CH, Wang J (2015) Permanent deformation characteristics of saturated sand under cyclic loading. Can Geotech J 52(6):1–13. doi:10.1139/cgj-2014-0341

Cerni G, Cardone F, Virgili A, Camilli S (2012) Characterisation of permanent deformation behaviour of unbound granular materials under repeated triaxial loading. Constr Build Mater 28(1):79–87. doi:10.1016/j.conbuildmat.2011.07.066

Chen C, Indraratna B, McDowell G, Rujikiatkamjorn C (2015) Discrete element modelling of lateral displacement of a granular assembly under cyclic loading. Comput Geotech 69:474–484. doi:10.1016/j.compgeo.2015.06.006

Cuéllar P, Mira P, Pastor M, Merodo JAF, Baeßler M, Rücker W (2014) A numerical model for the transient analysis of offshore foundations under cyclic loading. Comput Geotech 59:75–86. doi:10.1016/j.compgeo.2014.02.005

Danne S, Hettler A (2015) Experimental strain response-envelopes of granular materials for monotonous and low-cycle loading processes. In: Triantafylidis TH (ed) Holistic simulation of geotechnical installation processes. Springer International Publishing, Berlin-Heidelberg, pp 229–250

Daum M (2008) Simplified presentation of the stress-energy method for general commercial use. J Test Eval 36(1):100–102. doi:10.1520/JTE101202

Desai CS, Siriwardane HJ (1984) Constitutive laws for engineering materials with emphasis on geologic materials. Prentice-Hall, New Jersey

EN 13286-7 (2004) European Committee for Standardization. Unbound and hydraulically bound mixtures – Part 7: cyclic load triaxial test for unbound mixtures

Fadaee MJ, Saffari H, Tabatabaei R (2008) Shear effects in shakedown analysis of offshore structures. J Ocean Univ China 7(1):77–83. doi:10.1007/s11802-008-0177-z

Feng J, Wu XY, Zhu BL, Yang QX (2015) Analytical solution to one-dimensional consolidation in unsaturated soils under sinusoidal cyclic loading. J Cent South Univy 22:646–653. doi:10.1007/s11771-015-2566-y

Goldscheider M. (1978) Shakedown and incremental collapse of structures in dry sand bodies. In: Proceedings of dynamical methods in soil and rock mechanics, plastic and long-term effects in soils, Balkema, Rotterdam, 2

Green RA, Mitchell JK, Polito CP (2000) An energy-based excess pore pressure generation model for cohesionless soils. In: Proceedings of the Developments in Theoretical Geomechanics—The John Booker Memorial Symposium, Australia, 1–9

Gu C, Wang J, Cai Y, Yang Z, Gao Y (2012) Undrained cyclic triaxial behavior of saturated clays under variable confining pressure. Soil Dyn Earthq Eng 40:118–128. doi:10.1016/j.soildyn.2012.03.011

Jain A, Veas JM, Straesser S, Van Paepegem W, Verpoest I, Lomov SV (2015) The master sn curve approach–a hybrid multi-scale fatigue simulation of short fiber reinforced composites. Compos Part A. doi:10.1016/j.compositesa.2015.11.038

Kalinowska M, Jastrzębska M (2014) Behaviour of cohesive soil subjected to low-frequency cyclic loading in strain-controlled tests. Studia Getechnica et Mechanica 36(3):21–35. doi:10.2478/sgem-2014-0024

Karg C, François S, Haegeman W, Degrande G (2010) Elasto-plastic long–term behavior of granular soils: modelling and experimental validation. Soil Dyn Earthquake Eng 30(8):635–646. doi:10.1016/j.soildyn.2010.02.006

Kokkali P, Anastasopoulos I, Abdoun T, Gazetas G (2014) Static and cyclic rocking on sand: centrifuge versus reduced–scale 1 g experiments. Géotechnique 64(11):865–880. doi:10.1680/geot.14.P.064

Kokusho, T., and Y. Kaneko (2014), Dissipated & Strain Energies in Undrained Cyclic Loading Tests for Liquefaction Potential Evaluations, In: Proceedings of the tenth National Conference in Earthquake Engineering, Earthquake Engineering Research Institute, Anchorage, 1–10

Kokusho T, Ito F, Nagao Y, Green RA (2012) Influence of non/low–plastic fines and associated aging effects on liquefaction resistance. J Geotech Geoenviron Eng ASCE 138(6):747–756. doi:10.1061/(ASCE)GT.1943-5606.0000632

König JA, Maier G (1981) Shakedown analysis of elastoplastic structures: a review of recent developments. Nucl Eng Des 66(1):81–95. doi:10.1016/0029-5493(81)90183-7

Koseki J, Mikami T, Sato T (2014) Deformation characteristics of granular materials in cyclic one-dimensional loading tests. Transport Infrastruct Geotechnol 1(1):54–67. doi:10.1007/s40515-014-0002-7

Li LL, Dan HB, Wang LZ (2011) Undrained behavior of natural marine clay under cyclic loading. Ocean Eng 38(16):1792–1805. doi:10.1016/j.oceaneng.2011.09.004

Liang C, Liu T, Xiao J, Zou D, Yang Q (2015) Effect of stress amplitude on the damping of recycled aggregate concrete. Materials 8(8):5298–5312. doi:10.3390/ma8085242

Lu Z, Yao HL, Liu J, Hu Z (2014) Experimental evaluation and theoretical analysis of multi–layered road cumulative deformation under dynamic loads. Road Mat Pavement Des 15(1):35–54. doi:10.1080/14680629.2013.852609

Nega A, Nikraz H, Al-Qadi IL (2015) Simulation of shakedown behavior for flexible pavement's unbound granular layer. In: Harvey J, Chou KF (eds.) Airfield and Highway Pavements, pp 801–812. doi: 10.1061/9780784479216.071

Ostadan F, Deng N, Arango I (1996) Energy-based method for liquefaction potential evaluation, phase I Feasibility study U.S. Department of Commerce, Technology Administration, National Institute of Standards and Technology, Building and Fire Research Laboratory, San Francisco, pp 96–701

Panoskaltsis VP, Bahuguna S (1996) Micro and macromechanical aspects of the behavior of concrete materials with special emphasis on energy dissipation and on cyclic creep. J Mech Behav Mat 6(2):119–134. doi:10.1515/JMBM.1996.6.2.119

Pasik T, Chalecki M, Koda E (2015) Analysis of embedded retaining wall using the subgrade reaction method. Studia Geotechnica et Mechanica 37(1):59–73. doi:10.1515/sgem-2015-0008

PN–CEN ISO/TS 17892-4:2009, Polish committee for standardization. geotechnical investigations—Soil Laboratory Testing—Part 4: Sieve Analysis, Polish Committee for Standardization: Warsaw, Poland, 2009

PN–EN 13286:2010/AC, Polish Committee for Standardization. Unbound and hydraulically bound mixtures—Part 2: Testing methods for laboratory reference density and water content—Proctor compaction; Polish Committee for Standardization: Warsaw, Poland, 2010

PN–EN ISO 14688-2:2006, Polish Committee for Standardization. Geotechnical Investigations—Soil Classification—Part 2: Classification Rules, Polish Committee for Standardization: Warsaw, Poland, 2006

Puppala AJ, Saride S, Chomtid S (2009) Experimental and modeling studies of permament strains of subgrade soils. J Geotech Geoenviron Eng 135(10):1379–1389. doi:10.1061/(ASCE)GT.1943-5606.0000163

Sas W, Głuchowski A, Szymański A (2014) Impact of the stabilization of compacted cohesive soil–sandy clay on field criterion improvement. Ann Warsaw Univ Life Sci 46(2):139–151. doi:10.2478/sggw-2014-0012

Sas W, Głuchowski A, Radziemska M, Dzięcioł J, Szymański A (2015) Environmental and geotechnical assessment of the steel slags as a material for road structure. Materials 8(8):4857–4875. doi:10.3390/ma8084857

Seo J, Kim YC, Hu JW (2015) Pilot Study for investigating the cyclic behavior of slit damper systems with recentering shape memory alloy (SMA) bending bars used for seismic restrainers. Appl Sci 5(5):187–208. doi:10.3390/app5030187

Sharp RW, Booker JR (1984) Shakedown of pavements under moving surface loads. J Transport Eng 110:1–14. doi:10.1061/(ASCE)0733-947X(1984)110:1(1)

Soares R, Allen D, Little DN Berthelot CA (2014) Multi–scale computational mechanics model for predicting rutting in asphaltic pavement subjected to cyclic mechanical loading. In: Transportation Research Board 93rd Annual Meeting DC, USA. Accessed 12–16 Jan 2014 pp 1–17

Soliman H, Shalaby A (2015) Permanent deformation behavior of unbound granular base materials with varying moisture and fines content. Transport Geotech 4:1–12. doi:10.1016/j.trgeo.2015.06.001

Sun L, Gu Ch, Wang P (2015) Effects of cyclic confining pressure on the deformation characteristics of natural soft clay. Soil Dyn Earthquake Eng 78:99–109. doi:10.1016/j.soildyn.2015.07.010

Tang LS, Chen HK, Sang HT, Zhang SY, Zhang JY (2015) Determination of traffic-load-influenced depths in clayey subsoil based on the shakedown concept. Soil Dyn Earthquake Eng 77:182–191. doi:10.1016/j.soildyn.2015.05.009

Tao M, Mohammad LN, Nazzal MD, Zhang Z, Wu Z (2010) Application of shakedown theory in characterizing traditional and recycled pavement base materials. J Transport Eng 136(3):214–222. doi:10.1061/(ASCE)0733-947X(2010)136:3(214)

Tasdemir Y, Das PK, Brigisson B (2010) Determination of mixture fracture performance with the help of fracture mechanics. In: Proceedings of Ninth International Congress on Advances in Civil Engineering, Sept 2010, Turkey, 1–7

Werkmeister S (2003) Permanent deformation behavior of unbound granular materials. Ph.D. dissertation. University of Technology, Dresden, Germany

Werkmeister S (2006) Shakedown analysis of unbound granular materials using accelerated pavement test results from New Zealand's CAPTIF facility. Pavement Mech Perf 154:220–228. doi:10.1061/40866(198)28

Werkmeister S, Dawson A, Wellner F (2001) Permanent deformation behavior of granular materials and the shakedown concept. Transport Res Record 1757:75–81. doi:10.3141/1757-09

Wichtmann T (2005) Explicit accumulation model for non-cohesive soils under cyclic loading. Ph.D. Thesis, Ruhr-University Bochum

Zhang Z, Roque R, Birgisson B, Sangpetngam B (2001) Identification and verification of a suitable crack growth law. J Assoc Asphalt Paving Technol 70:206–241

Zhou J, Gong XN (2001) Strain degradation of saturated clay under cyclic loading. Can Geotech J 38(1):208–212. doi:10.1139/cgj-38-1-208